Source Analysis of Median Nerve and Finger Stimulated Somatosensory Evoked Potentials: Multichannel Simultaneous Recording of Electric and Magnetic Fields Combined with 3D-MR Tomography

Helmut Buchner*, Manfred Fuchs+, Hans-Aloys Wischmann+, Olaf Dössel+, Irene Ludwig*, Achim Knepper@, and Patrick Berg#

Summary: At the current state of technology, multichannel simultaneous recording of combined electric potentials and magnetic fields should constitute the most powerful tool for separation and localization of focal brain activity. We performed an explorative study of multichannel simultaneous electric SEPs and magnetically recorded SEFs. MEG only sees tangentially oriented sources, while EEG signals include the entire activity of the brain. These characteristics were found to be very useful in separating multiple sources with overlap of activity in time. The electrically recorded SEPs were adequately modelled by three equivalent dipoles located: (1) in the region of the brainstem, modelling the P14 peak at the scalp, (2) a tangentially oriented dipole, modelling the N20-P20 and N30-P30 peaks, and part of the P45, and (3) a radially oriented dipole, modelling the P22 peak and part of the P45, both located in the region of the somatosensory cortex. Magnetically recorded SEFs were adequately modelled by a single equivalent dipole, modelling the N20-P20 and N30-P30 peaks, located close to the posterior bank of the central sulcus, in area 3b (mean deviation: 3 mm). The tangential sources in the electrical data were located 6 mm on average from the area 3b. MEG and EEG was able to locate the sources of finger stimulated SEFs in accordance with the somatotopic arrangement along the central fissure. A combined analysis demonstrated that MEG can provide constraints to the orientation and location of sources and helps to stabilize the inverse solution in a multiple-source model of the EEG.

Key words: Somatosensory evoked potentials; Source analysis; Simultaneous magnetic and electric recording.

Introduction

The current sources of electrically stimulated somatosensory evoked potentials (SEPs) have been a matter of discussion since the early sixties (Broughton 1969). There is wide agreement about the generator sources of the scalp recorded peak P14 in the brainstem, and the N20-P20 in the posterior bank of the central sulcus. The central P22 has been attributed to a source at the crown of either the first precentral or the postcentral gyrus (Allison et al. 1991; Desmedt 1988).

On the other hand, there is only speculation about the sources contributing to later peaks of the SEPs. Several authors have suspected generators in the motor cortex or supplementary motor area, which may contribute to the frontal N30 (Desmedt and Tomberg 1989; Rossini et al. 1989).

At the current state of technology, multichannel simultaneous measurements of both electric potentials and magnetic fields provide the most powerful tool for separation and localization of focal brain activity (Lopes da Silva et al. 1991). Multichannel electrical measurement provides information about the entire activity of the brain, including deep and radially oriented sources (Nunez 1990). Multichannel magnetic measurements provide the most accurate localization of tangentially oriented, superficially located sources (Hari et al. 1991).

The combination of both technologies with 3D-MR-tomography may yield further information about the generators of the SEP.

To our knowledge we have performed the first simultaneous multichannel recordings of electric and magnetic fields combined with 3D-MR-tomography. The study had several aims: (1) To learn how to record simultaneous electric and magnetic data, (2) to determine how to analyze the data, and (3) to develop further hypotheses about the generators of the SEPs and SEFs.

*Department of Neurology, RWTH Aachen.
+Philips GmbH Forschungslaboratorien, Technical Systems Department, Hamburg.
@Institute of Measurement Technology, RWTH Aachen.
#Department of Psychology, University of Konstanz.
Accepted for publication: January 25, 1994.
Correspondence and reprint requests should be addressed to Helmut Buchner, M.D., Department of Neurology, Klinikum RWTH, Pauwelsstr. 30, D-52057 Aachen, FRG.

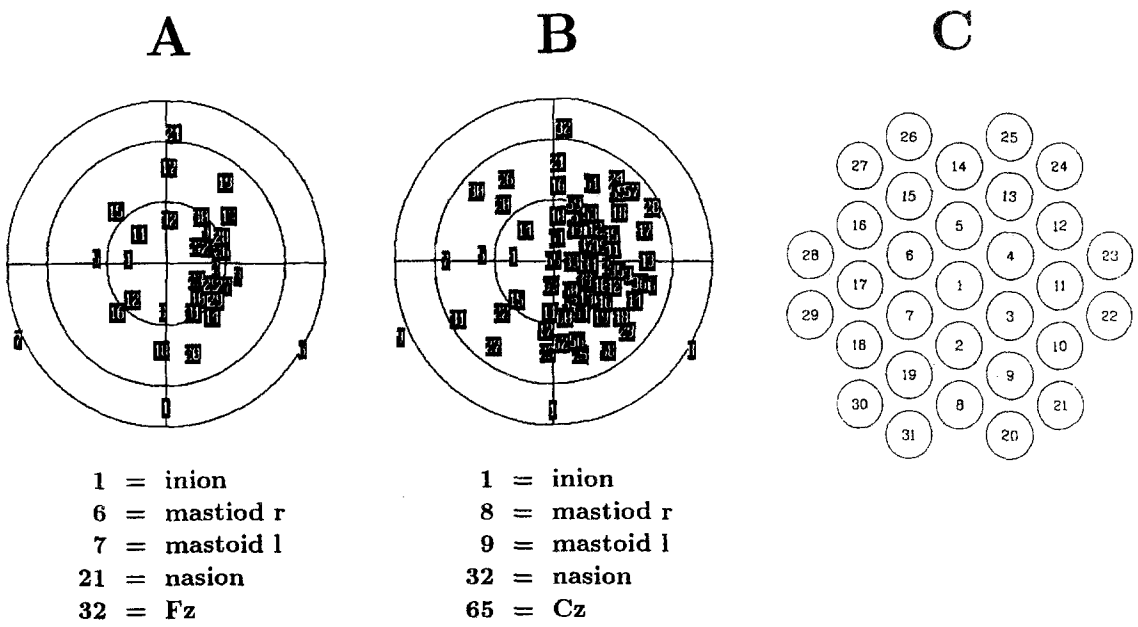

Figure 1. Electrode locations shown in a top meridian projection around Cz in 31-channel (A) and 64-channel recordings (B), subject IL. MEG system positions in a projection through the centre at #1 (C).

Material and Method

Three healthy subjects (AM, HB, IL, two females, age 26, 28 and 39 years) were studied in the magnetically shielded room of the Philips Research Laboratories, Hamburg. During the measurements, the subject lay with the head fixated by a vacuum cast. All subjects gave their informed consent.

The left median nerve was stimulated at the wrist with an intensity of twice the motor threshold. The first, third and fifth finger were stimulated independently with ring electrodes fixed at the first and third interphalangeal joint with an intensity of twice the sensory threshold. Pulses were rectangular with a duration of 0.2 ms and a frequency of 3.1/s.

Recordings were performed simultaneously with a 31-channel first-order gradiometer and a 31-channel electrode array (Dössel et al. 1991, 1992, 1993). Two Nicolet SM 2000 amplifiers and the Scan software (NeuroScan, Herndon, VA) were used for data acquisition. Signals were sampled with 256 points over a sweep time of 128 ms pre- and 128 ms poststimulus (1 kHz sampling rate). Data were filtered below 5 and above 250 Hz. Four replications of 500 or 1000 sweeps were averaged online.

Electric SEPs were recorded from 31 scalp electrodes (Ag-AgCl sintered, impedance below 5 kOhm) as shown in figure 1a. Electrodes were placed closer together over the stimulated hemisphere. The reference was at Fz. Additional 64-channel electric SEPs were recorded from subject AM and IL (figure 1b), using a Cz reference. Identical experimental conditions were used.

The MEG-system had an arrangement of 31-channels (figure 1c), (first order two turn gradiometer, 20 mm diameter, 70 mm base length, with an outer diameter of 132.5 mm). The overall system noise was below 10 fT/Hz1/2 (Dössel et al. 1993). The SEFs were recalibrated and cross talk corrected. The position of the MEG-system was adjusted in such a way that the tangential source around 20 ms latency (N20-P20) was located at its centre, using replicated test measurements of the median nerve SEFs. The exact position of the MEG system relative to the head was determined using four coilsets placed on the scalp (figure 2) (Fuchs et al. 1992). This system was found to have a localization deviation of less than 2 mm. The head position was measured twice, before and after each recording, in order to control the position of the head.

MR recordings were made on a different day from the combined EEG/MEG recordings. After data acquisition, EEG electrode and coilset positions were marked using a felt-tip marker. Before MR recording, these marks were used to locate where small wooden discs should be fixed to the scalp. The discs had a hole filled with fat in order to make the electrode and coilset positions visible on the 3D-MR images. To distinguish electrodes from coilsets, the holes were 3 mm in diameter for electrodes, and 5 mm for coilsets. For one subject (AM), marker positions were not available for MR. 64-channel EEG recordings were acquired on the same day as the MR. The wooden disks were attached immediately after recording.

MR were performed with a 1.5 T superconducting

Figure 2. 3D-surface reconstruction of the MR with electrode and coil position markers, subject IL.

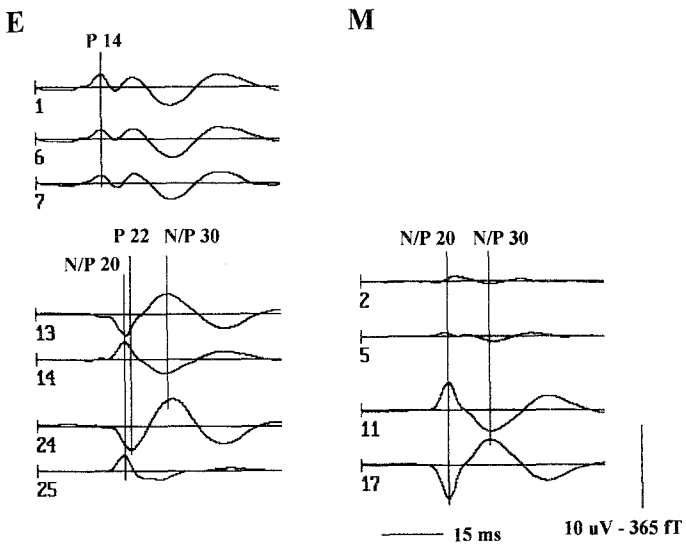

Figure 3. Median nerve stimulated SEPs, 4000 averages, in simultaneous 31-channel electric average referenced (E) and magnetic (M) recording, subject IL. Waveforms at selected electrodes are shown, for electrode positions see figure 3.

magnet and a circular polarized head coil. After parallel alignment of the interhemispheric plane of the brain with the sagittal imaging plane, a strongly T1-weighted gradient echo pulse sequence (fast low-angle shot) was applied. For all MRs the technical factors were 40 ms repetition time, 5 ms echo time, 40 degree flip angle, one excitation, 300 mm field of view, and a 256 x 256 image matrix. This resulted in 128 slices with a thickness of 1.56 mm and a pixel size of 1.17 by 1.17 mm.

Data analysis

MRs were read into the anatomic display software package of the MEG-Software (Philips Research Laboratories). A surface reconstruction of the head was generated for optimal visualization of the positions of the electrodes and coil markers (figure 2). The cartesian coordinates of the electrode markers were assigned to each amplifier channel, read into a file and transferred to an IBM-compatible PC. A separate PC program was used to perform a least squares fit for the sphere best fitting the 3D electrode cloud. The centre of the sphere and its radius were computed in MR coordinates. The distance of each electrode from the centre was then set to the radius of the sphere. A coordinate system was defined closely related to the standard 10-20 system of electrode placement: The Z-axis was defined by a vector connecting the centre of the sphere and the Cz electrode, the electrode at the inion (#1) then defined the Y-Z-plane. Thus, the Y-axis pointed anteriorly towards Fpz and the X-axis laterally towards T4. Finally, electrode positions were transformed into the spherical coordinate system of the BESA program (Brain Electric Source Analysis, NeuroScan, Herndon, VA). The cartesian coordinates of the coilset markers were assigned to each coilset number and used to determine the exact position of the MEG system relative to the head.

Preprocessing of the electric and magnetic signals: first, electric and magnetic signal files containing reproduced measurements recorded in constant head positions were averaged. Second, the time interval between zero and 8 ms, containing the stimulus artifact, was set to zero, and signals were baseline corrected by subtracting the mean signal from minus 128 ms to 0 ms. Third, data were digitally filtered (high pass: 20 Hz, 12 dB/oct and low pass: 250 Hz, 24 dB/oct forward filtered) in order to enhance the signal to-noise ratio and to reduce the overlap of low-frequency components. This overlap, if not removed by filtering, can lead to substantial dipole mislocation. Also, most of the energy of the early SEPs is contained in this frequency band (Lüders et al. 1983, 1986). Figure 3 shows electric and magnetic median nerve SEP/SEFs from one of the subjects.

Next, the global field power (GFP) was computed (Lehmann 1987) (figure 4).

The signal-to-noise ratios (SNR) were computed separately for each electric and magnetic channel. The SNR was defined as follows: The average over all absolute amplitudes in the signal interval minus the average over all absolute amplitudes in the prestimulus interval (-128 to 0 ms), vs. the average over all absolute

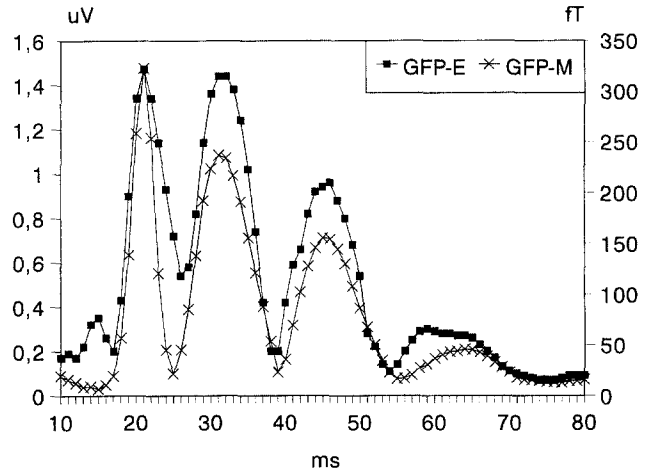

Figure 4. Global field power from simultaneous electric (GFP-E) and magnetic (GFP-M) recording of median nerve SEPs, subject IL. Data shown in figure 3.

amplitudes in the prestimulus interval.

Instantaneous spline interpolated maps were computed at each sampling point between 10 ms and 80 ms (Giard et al. 1985). Electric potential maps were displayed at the 3D-surface reconstruction of the 3D-MR. Magnetic field maps were displayed at the position of the hexagonal concave arrangement of the lower pickup coils of the MEG-system (figure 5).

An approximated 3-shell spherical head model was used to obtain various electric dipole source models for each SEP data set (Scherg 1990, 1992; Fender 1991). All computations were performed using the measured electrode positions. Source locations computed in a sphere of 85 mm radius were adjusted to the radius of the fitted sphere and transformed to MR-coordinates.

A spherical head model was used for magnetic source analysis. The radius and the centre of the sphere were determined as follows: First, a sphere with a radius and centre best fitting the surface of the whole head (least squares fit) was taken and the location of a single equivalent dipole was computed at the latency of the N20 peak. Next, a segment of the head defined by a plane orthogonal to the longitudinal axis of the MEG-system and 20 mm below the source was taken and a sphere was fitted to this segment of the head surface. The thickness of the segment was not critical: Sources computed in spheres defined in segments with depths varying between that of the source to the source depth plus 40 mm showed locations differing by not more than 1 mm in each axis.

Several strategies of dipole source analysis were applied, without any additional assumptions, to achieve a generator model on the basis of electric and magnetic data:

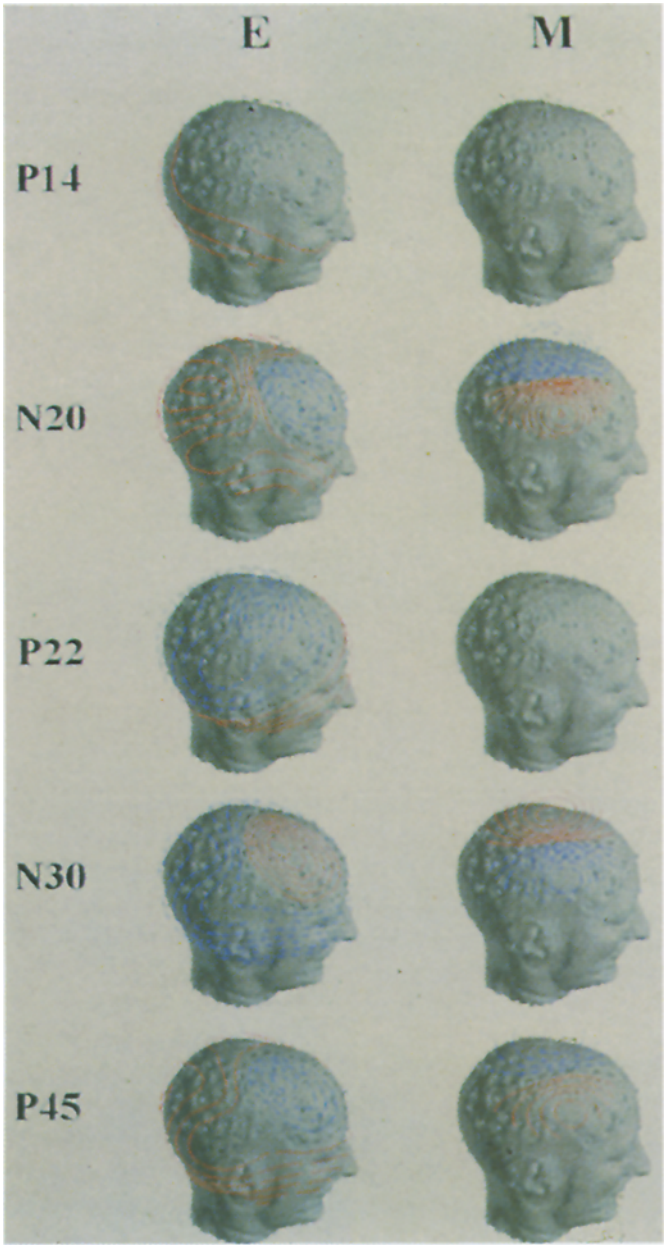

Figure 5. Maps of median nerve stimulated SEPs, data are shown in figure 3. Potential maps shown on the surface of the head (E). Magnetic field maps shown on the sensor surface of MEG system (M). Maps were computed at the maxima of GFP (see figure 4) and at the maximum radial activity of the electric field around 22 ms.

1. A single instantaneous dipole model (moving dipole) was computed at each digitization point between 10 and 80 ms post-stimulus.

2. A single spatio-temporal dipole model with fixed location but varying orientation and amplitude in time (regional source) was applied. The computations were

Table I. Signal-to-noise ratio in simultaneously recorded 31-channel electric and magnetic data. The best signal-to-noise ratio in one of the channels is shown, computed in the epoch of 10-128 ms poststimulus, in the epoch of 10 ms around the N20 peak and at the time points of maximum GFP (P1 around 20 ms, P2 around 32 ms, P3 around 45 ms).

signal-to-noise ratio in electric and magnetic recording										
	10-128 ms		N20+/- 5 ms		P1		P2		P3	
	E	M	E	M	E	M	E	M	E	M
AM										
ME	6.1	8.8	7.0	15.0	10.3	46.6	18.4	47.3	18.4	31.2
I	6.3	7.6	5.2	8.2	4.7	17.0	10.2	19.4	3.6	7.3
III	4.1	12.3	2.8	20.0	6.5	41.2	10.8	58.7	7.2	34.9
V	4.1	4.2	4.1	7.0	4.1	16.4	9.2	16.1	3.6	8.4
HB										
ME	9.5	9.4	6.8	20.3	8.0	46.0	8.0	31.1	19.7	31.1
I	2.7	2.5	3.2	2.8	4.5	4.8	2.5	4.3	3.8	4.4
III	7.0	6.0	3.2	6.9	3.1	10.0	1.2	11.9	1.4	2.3
V	4.5	4.0	2.1	4.0	2.9	7.9	3.0	4.2	5.6	11.6
IL										
ME	6.9	22.7	15.5	54.2	31.2	148.5	31.2	102.1	19.8	62.3
I	4.1	10.4	5.8	19.6	10.8	47.0	5.1	36.5	8.9	33.8
III	6.0	14.9	3.8	20.7	9.7	53.1	2.8	50.7	20.0	46.8
V	1.7	10.4	3.1	10.8	5.4	24.9	2.1	31.1	3.9	35.5

performed in the signal interval from 10 to 80 ms.

3. A multiple spatio-temporal dipole model (fixed dipole) was applied. Computations were performed using a sequential strategy, with epochs defined by the GFP, again in the interval from 10 to 80 ms.

Based on the equivalent dipole strength from the MEG, one can roughly estimate the size of the activated cortical layer (Lopes da Silva et al. 1991). The poles at the cortex were assumed to be separated by 1 mm, which is in the order of magnitude of the length of the soma and dendritic arborization of large pyramidal cells. The current density was assumed to be at an upper limit of 250 nA/mm^2 (Freeman 1975). The magnitude of a single instantaneous dipole computed at the time point of maximum field power around 20 ms post-stimulus was taken. The calculated size of the activated cortical layer was divided by the depth of the central sulcus, roughly measured on the individual MRs. This provided an estimate of the width of the activated region along the central sulcus.

Results

The position of the head was measured twice, before and after stimulation of the median nerve and each finger. The 3D-position of each coilset was determined. The head position of subject AM was very stable during all measurements, while subjects HB and IL moved their head positions more than 2 mm during some of the measurement blocks.

The SNR was computed in the signal epoch (10-128 ms), the first 10 ms of cortical activity (median nerve 18 to 28 ms, first and third finger 20 to 30 ms, fifth finger 22 to 32 ms) and at the time points of maximum global field power (P1 approximately 20 ms, P2 approximately 32 ms, P3 approximately 45 ms). The highest S/N ratio in both electric and magnetic data were taken, irrespective of the channel in which it was observed (table I). On average the SNR was three times higher in magnetic than in electric recordings (subject AM 3.0 +/- 3.8, HB 2.0 +/- 1.2, IL 5.6 +/- 4.1).

The GFP from both electric and magnetic data were compared by plotting both in the same figure (figure 4). Both electric and magnetic data showed three major peaks with almost identical latencies around 20 ms, 32 ms and 45 ms. Two major differences between electric and magnetic GFP were observed in all stimulation conditions:

1. The electric GFP started with a small first peak around 14 ms, which was not present in the magnetic GFP.
2. The minimum of the electric GFP around 24 ms was clearly different from zero, while the magnetic GFP were close to zero at this latency.

Maps were computed at the latencies of the GFP peaks and at the minimum of electric GFP around 25 ms (figure 5). The potential and field maps are displayed relative to

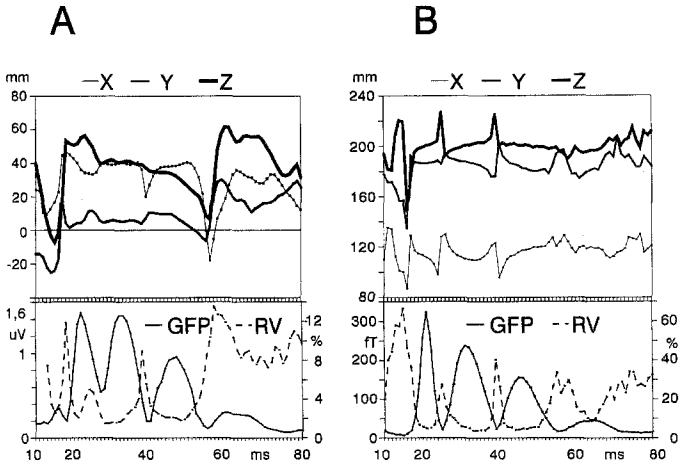

Figure 6. Cartesian coordinates of the single instantaneous dipoles computed on electric (A) and magnetic (B) data as a function of time (data shown in figures 3-5). Electric data were computed in the spherical head model of the BESA program. Magnetic data were computed in the spherical head model of the MEG software. The GFP and residual variance are also shown.

the subject's head. In all subjects the following results were obtained:

1. Around 14 ms, there was a wide spread positivity in the potential maps, while almost no signal was observed in the magnetic field data.
2. Around 20 ms, there was a clear bipolar field pattern in both recordings.
3. Around 25 ms, there was a monopolar radial field pattern in the potential maps, while almost no signal was observed in the field data.
4. Around 32 ms, there was a clear bipolar pattern in both recordings.
5. Around 45 ms, there was a bipolar pattern with pronounced negativity at the fronto-central region in the potential maps, while the field maps showed a clear bipolar pattern.

Dipole source analysis

Single instantaneous dipole model (moving dipole): in both electric and magnetic data a single instantaneous dipole model was computed. The coordinates of the source locations were plotted together with the unexplained variance of the data and the GFP (figure 6a, b). The electric sources were evaluated in the spherical head model of the BESA program and the magnetic sources in the spherical head model of the MEG software.

In general, the residual variance was large and the location of the dipole was unstable when the field power was low. In detail the following results were obtained:

1. A single source did not explain the electric field in the epoch between 20 and 25 ms, while the magnetic field was very well represented by this model (residual variance around 6%). An artificial current dipole probe is usually explained by the mathematical algorithm with a residual variance of around 3% due to noise. The electric sources showed variable locations in this epoch, while the magnetic sources were stable at one location.
2. A single source explained the electric and magnetic field in the epoch around the second maximum of GFP (around 32 ms).
3. A single source model explained the electric and magnetic field in the epoch around the third maximum of GFP (45 ms in the case of median nerve SEPs). The electric sources showed variable locations in this epoch, while the magnetic sources were stable at one location.

Single spatio-temporal fixed dipole model (regional source): a regional source, (i.e., a single dipole fixed in location but with variable orientation, Scherg and von Cramon 1986) was fitted in both electric and magnetic data. In general the following results were obtained:

1. In electric data a regional source computed in the epoch from 10 to 80 ms localized close to the location of the single instantaneous dipole at the time point of the second peak of GFP (around 32 ms in the case of median nerve SEPs). This deviated from the location of the single instantaneous dipole computed at the first and third peak of GFP (mean deviation = 10 mm). Hence, source location varied in time, although the explained variance of the data was above 80%.
2. In magnetic data a regional source fitted in the epoch from 10 to 80 ms localized close to the single instantaneous dipoles computed at the latency of the peaks of GFP (mean deviation = 2 mm). Hence, source locations were very stable across the three epochs around the maxima in GFP.

Multiple spatio-temporal dipole model (fixed dipole): a multiple dipole model with fixed locations and orientations but varying amplitudes of each dipole source was computed in the electric and magnetic data (Scherg and von Cramon 1985; Scherg 1990, 1992; Fender 1991). In electric data a similar strategy for dipole location of median nerve and finger stimulated SEPs was applied in 31-channel and 64-channel recorded data:

1. A regional source was fitted in the first epoch around the first maximum of GFP (14 ms).
2. A second regional source was fitted in the second epoch, while the location of the first regional source was

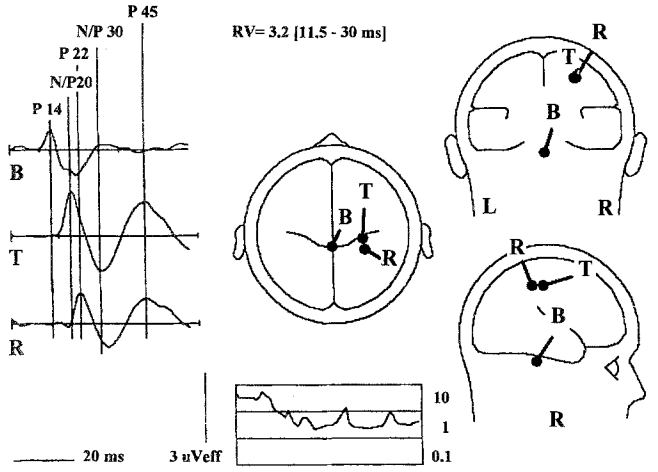

Figure 7. Multiple spatio-temporal dipole model of electric data, computed in the interval between 10 and 60 ms poststimulus. On the bottom the residual variance in time is depicted in a logarithmic scaling. Data shown in figures 3-6.

held constant.

3. The orientation of the first dipole of each regional source was adjusted to explain the current flow at the maximum effective voltage explained by the regional dipole sources. The second and third dipole of the first regional source and the third dipole of the second regional source were switched off, because they explained less then 10% of the activity. This did not substantially increase the unexplained variance of the data.

4. The orientation and location of the remaining two dipoles of the second regional dipole source were fitted in the second epoch defined by GFP (around 20 ms), while the first dipole was held constant.

5. A test regional dipole source was added and its location was fitted in order to test whether there was additional unexplained activity in other brain regions.

The resulting model consists of three dipole sources (figure 7): The first (B = brainstem) at the lower half of the head model, the second (T = tangential) and third (R = radial) at the upper right quadrant of the head model. These three dipole sources explained 90 to 98.5% of the variance of the data in the whole epoch after the stimulus. The test source detected no significant additional activity.

The dipole model indicates considerable overlap of activity generated at different locations in the brain:

1. The P14 field at the scalp was modelled by a single dipole (B) located in the region of the brainstem.

2. The N20-P20 field at the scalp was modelled by a tangentially oriented source (T) located in the region of the somatosensory cortex, with additional overlapping activity of the brainstem source (B).

3. The P22 field at the scalp was modelled by a radially oriented source (R) located in the region of the cortex, with additional activity of the B and T sources.

4. The N30-P30 field at the scalp was modelled by the T source. The R source showed no or very little activity at this latency time.

5. The P45 field was modelled by both the T and R sources.

In the magnetic data, a single fixed dipole computed in the epoch between 10 and 80 ms post-stimulus located close to the single instantaneous dipoles computed at the latency of the peaks of GFP (mean deviation = 3.5 mm), and close to the single dipole fixed in location but variable in orientation (regional source) (mean deviation = 2.9 mm).

Source location relative to anatomy

The coordinates of the source locations computed from electric and magnetic data were converted to the coordinate system of the MRs (table II). For the magnetic data, locations computed with a single instantaneous dipole model at the time point of maximum GFP around 20 ms (N20) were used. In the case of electric data (both 31- and 64-channel recordings) locations of the T-source computed with the multiple spatio-temporal dipole model were used. Two major problems appeared using this procedure:

1. Subjects HB and IL (stimulation of the first finger) moved their heads several millimeters relative to the MEG-system during one sequence of data acquisition. Hence, the locations of the computed magnetic sources relative to the anatomy were uncertain.

2. As stated above, a reliable position of the head relative to the MEG-system could not be determined in subject AM. On the other hand, analysis of the relative source locations was not affected, because subject AM showed a very stable position of the head during the measurements.

These problems did not occur in the 64-channel electric recording from subjects AM and IL.

In datasets without these problems (see table II) a pseudo-3D reconstruction of the 3D-MR was used to decide whether circles of 3, 6 and 9 mm drawn around the locations of the sources intersected the posterior bank of the central sulcus (table II, figure 8).

The central sulcus was identified on the basis of anatomical landmarks, both in axial and sagittal reconstructions of the 3D-MR. In axial images the central

Table II. Source locations and 3D-MR. The T dipole source location of the multiple spatio-temporal source model of the electric data (31-channel E-31 and 64-channel E-64), and the instantaneous dipole source location computed at the latency of the first maximum of GFP (20 ms) in the magnetic data. All values are in millimeters in MR coordinates (X-axis from frontal to occipital, Y-axis from caudal to rostral, Z-axis from right to left). The deviation of the sources from the posterior bank of the central sulcus (Dev.-CS) are presented in steps of below 3, 6 and 9 mm. Magnetic source localization within the 3D-MR was not possible in subjects AM and HB.

location of sources and 3D-MR MR-coordinates - all in mm							
		AM		HB	IL		
		E-64	E-31	E-31	E-64	E-31	M
ME	x	116	116	110	115	108	112
	y	143	137	168	188	184	187
	z	226	213	208	199	197	202
	Dev.-CS	6	-	3	3	3	3
I	x	115	113	119	111	111	108
	y	138	126	177	179	179	183
	z	220	203	207	195	195	199
	Dev.-CS	9	-	9	6	6	3
III	x	116	108	113	119	119	118
	y	143	129	170	189	189	185
	z	225	221	115	199	199	202
	Dev.-CS	6	-	3	3	3	3
V	x	119	113	118	119	119	116
	y	146	124	171	185	185	187
	z	232	208	116	199	200	204
	Dev.-CS	9	-	3	3	3	3

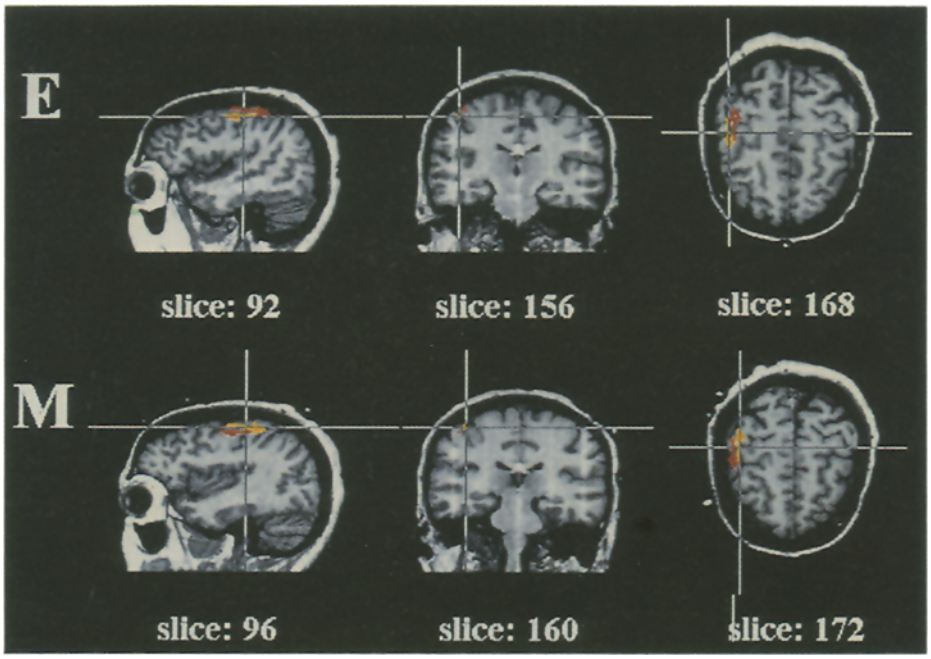

Figure 8. Dipole sources projected onto the MR, shown in a pseudo-3D image. The T source location from the multiple spatio-temporal dipole model of the electric data (E, yellow arrow) and the instantaneous dipole source location computed at the latency of the N20 maximum of GFP in the magnetic data (M, yellow arrow) are shown. For comparison, the red arrow shows the source computed in the other type of measurement, i.e., the magnetic source in E and the electric source in M. Source location is at the midpoint of the arrow.

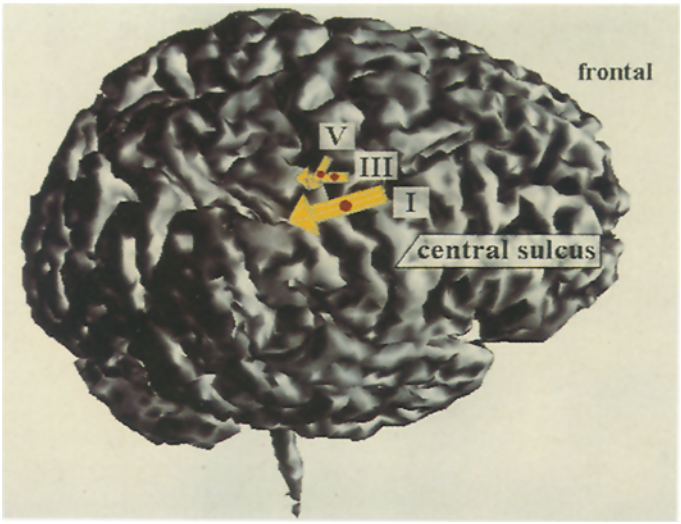

Figure 9. Reconstruction of the surface of the brain of subject IL. Magnetic sources localization of the finger stimulated N20 peaks were displayed. Orientations were indicated by a yellow arrow and locations by a red dot. The sources located in accordance to the somatotopic arrangement along the central sulcus. Notice the approximately orthogonal orientation of the sources relative to the bending of the central sulcus.

Table III. Magnitude of a single instantaneous dipole computed at the time point of maximum field power around 20 ms post-stimulus. Estimated area of the activated cortex, and its width on the central sulcus.

	Size of activated cortex		
	magnitude of dipole -nAm-	size of area -mm^2-	width on central sulcus -mm-
AM - depth of central sulcus 18 mm			
ME	34.1	136.4	7.6
I	10.0	40.0	2.2
III	15.1	60.4	3.4
V	6.4	25.6	1.4
HB - depth of central sulcus 17 mm			
ME	30.2	120.8	7.1
I	11.0	44.0	2.6
III	10.0	40.0	2.4
V	13.1	52.4	3.1
IL - depth of central sulcus 23 mm			
ME	69.7	278.8	12.1
I	25.8	103.2	4.5
III	19.4	77.6	3.4
V	13.2	52.8	2.3

sulcus was identified by the spatial configuration of the superior frontal, the precentral, the central, and the postcentral sulci (Eberling et al. 1989). In midsagittal images the central sulcus was defined as the first frontal sulcus relative to the vertical ramus of the cingulate sulcus and was followed in sequent images in the lateral direction.

The source locations from the magnetic data (subject IL) all located within 3 mm of the posterior bank of the central sulcus.

The source locations from the electric data from subject IL all located within 6 mm of the central sulcus. Source locations from electric data (64-channel recording) from subject AM were all within 9 mm of the central sulcus, and from subject HB (31-channel recording) within 3 mm, except the first finger source, which located 9 mm from the central sulcus.

In addition, it was evaluated whether the finger stimulated sources corresponded to the somatotopic arrangement along the central sulcus. In subject IL a clear somatotopic arrangement of the fingers was found in magnetic data (figure 9) and in the electric source locations. In subject AM (64-channel electric and 31-channel magnetic recording) a clear somatotopic arrangement of the fingers was obtained. In subject HB (31-channel electric and magnetic data) no somatotopic arrangement of the fingers was observed.

Table III presents the magnitude of single instantaneous dipoles computed at the time point of maximum field power around 20 ms post-stimulus, the estimated area of the activated cortical layer, and of the width of this region on the central sulcus. The area of the activated cortex after median nerve and finger stimulation was found to be very variable. The width of the finger representation area along the central sulcus varied between 4.5 mm after stimulation of the first finger and 1.4 mm after stimulation of the fifth finger (mean = 2.8 mm).

Discussion

A discussion on the localization accuracy of EEG and MEG was initiated by Cohen et al. (1990), leading to contrary opinions about the value of MEG-source analysis. Our results demonstrate that a focus on localization accuracy ignores other characteristics of EEG and MEG, which are very useful in source analysis of SEPs and SEFs.

Theoretically, two differences between EEG and MEG signals can be predicted: (1) Radially oriented sources or source components are not seen by MEG, (2) sources located beyond a depth of approximately 70 mm or more are seen by MEG with attenuated amplitudes (Cuffin and Cohen 1979; Cohen and Cuffin 1983; Hari 1991; Lopes da Silva et al. 1991). On the other hand, EEG signals include all the electric activity, because of the volume conductor

characteristics of the head.

Thus, in the case of early SEPs, the brainstem source giving rise to P14 and the radial source generating P22 were not seen by MEG (figures 3, 4, 5). The selection of tangentially oriented sources, provided by MEG, was found to be very useful in separating and locating multiple sources. Multiple sources were necessary to model the electrical data, while only one source accurately modelled the magnetic data (figures 4, 5, 6, 7) (Tiihonnen et al. 1989; Buchner and Scherg 1990; Baumgartner et al. 1991a, b; Franssen et al. 1992; Buchner et al. 1993).

Several results of our study were based on this difference between EEG and MEG: (1) The signal-to-noise ratio was found to be on average three times higher in MEG than in EEG recordings. MEG signals exclude activity from artifact sources with radial orientation and from those located at a distance of more than approximately 90 mm from the lower gradiometer coils (table I). (2) The location of a single instantaneous dipole source in MEG data was found to be almost identical at different points in time (distances between the locations averaged less than 2 mm) (figure 6b). (3) A single dipole source did not model the EEG-data (figure 6a). (4) A spatio-temporal dipole model separated multiple sources, with considerable temporal overlap of activity (figure 7).

Creating a multiple spatio-temporal dipole model was found to be relatively simple in the case of the early SEPs. This is because prior knowledge was available: (1) There has to be a source located at the brainstem, peaking around 14 ms, (2) there has to be a tangentially oriented source in the region of the somatosensory cortex, peaking around 20 ms, and (3) a radially oriented source peaking around 22 ms (Desmedt et al. 1987; Allison et al. 1991). However, there is no prior knowledge concerning the number of sources and their location and orientation in later time range of the SEP. Although the spatio-temporal dipole model provides the opportunity to separate multiple sources, the inverse problem is not uniquely solved (Achim et al. 1988; Scherg 1990; Nunez 1990; van Oosterom 1991; Scherg and Berg 1991). In this situation, separation of tangentially oriented sources using MEG may provide constraints to the number of sources and their locations and orientations in a multiple EEG source model (Cuffin and Cohen 1991).

Hypothesis about SEP generators

There is wide agreement about the generator sources of the early SEP components P14 and N20-P20. The central P22 was attributed to the precentral gyrus on the basis of scalp recorded data, but located at the postcentral gyrus on the basis of epicortical recordings (Desmedt 1988; Allison et al. 1991). There are a variety of speculations about the generators of the later potentials N30-P30 and P45.

The hypothesis of two radially oriented sources, one located frontally at the supplementary motor area generating the N30, and one located parietally at area 1, generating the P27, was supported by Desmedt and Tomberg (1989) and others (Rossini et al. 1989; Reilly et al. 1992; Cheron and Borenstein 1992). In our data, the MEG demonstrated a clear bipolar field pattern around 30 ms post-stimulus, at the time-point of the N30-P30 field in EEG maps. This field was well modelled by a single tangentially oriented dipole located at the posterior bank of the central sulcus, in both MEG and EEG data. No or very little radially oriented activity was found in the EEG data (figure 7). Hence, source analysis of simultaneous magnetic and electric recorded SEPs provides strong evidence for a single tangentially oriented generator of the scalp N30-P30 peaks, located at the area 3b and against the hypothesis of two radially oriented sources. This replicates early results of combined magnetic and electric recordings by Wood et al. (1985).

Several studies have demonstrated changes of the amplitudes either of the frontal N30 or the parietal P30 (labelled P27 by others) (Rossini et al. 1989; Cheron and Borenstein 1987, 1992; Reilly et al. 1992). This seems to support the dual radial hypothesis. However, this can also be explained by a change in orientation of the N30-P30 dipole due to pathological conditions or by additional radially oriented sources with significant activity only under the condition of interfering stimuli. Studies using simultaneous electric and magnetic recordings may provide further insight into the configuration of sources under such conditions.

The P45 potential was generated by both the radial and the tangential sources, demonstrated by the multiple dipole model of the EEG-data. MEG source analysis revealed a location of the tangential component at the location of the N20-P20 potential, in area 3b. This provides constraints for source localization in electric data using the spatio-temporal approach.

One advantage of MEG is that source current is directly measured and hence, the size of the activated brain region can be estimated on the basis of the magnitude of the equivalent dipole. The activated area was found to be very variable, but not its width on the central sulcus, which was in the range of 3 mm. This is in accordance with the distance between the thumb and the little finger observed in this study and by others (Baumgartner et al. 1991; Buchner et al. 1993). However, this is only a raw estimate, because amplitudes are also dependent on the synchrony and parallel arrangement of the activated neuronal population.

EEG and MEG source localization

We analyzed the electric and magnetic localization of the tangentially oriented dipole source of the N20 relative to the individual anatomy (figures 8, 9). The sources computed on electric recordings were all located within 9 mm of the posterior bank of the central sulcus. A prior study revealed locations on average below 6 mm from area 3b (Buchner et al. 1993). Sources computed on magnetic recordings located all within 3 mm of area 3b. However, source localization within the anatomy was only possible in one subject due to changes in the position of the head in one case and displacement of the coilsets used for measuring the head position in the other.

A complete somatotopic arrangement of the fingers was obtained in magnetic, and in electric source locations. Theoretically, the accuracy of source localization is probably better in magnetic than electric data (Hari et al. 1991, Williamson 1991), but this has to be proven in a study including more subjects. However, electric source localization was better than originally suspected, although the 3-shell spherical head model is only a simplified representation of the geometry and the resistive properties of the head tissues (Cuffin et al. 1990). This unexpected accuracy of electrical source localization may be caused by both the exact measurement of electrode positions on the head and the relatively good fits of the spheres to the head geometry in the parietal region. Electric source localization of generators in other brain regions might be more affected by the spherical head model, unless more accurate head models are available.

References

Achim, A., Richer, F. and Saint-Hilaire, J.M. Methods for separating temporally overlapping sources of neuroelectric data. Brain Topography, 1988, 1: 22-28.

Allison, T., McCarthy, G., Wood, C.C. and Jones, S.J. Potentials evoked in human and monkey cerebral cortex by stimulation of the median nerve. Brain, 1991, 114: 2465-2503.

Baumgartner, C., Barth, D.S., Levesque, M.F. and Sutherling, W.W. Functional anatomy of human hand sensorimotor cortex from spatio temporal analysis of electrocorticography. Electroenceph. Clin. Neurophysiol., 1991, 78: 56-65.

Baumgartner, C., Doppelbauer, A., Deecke, L., Barth, D.S., Zeitlhofer, J., Lindinger, G. and Sutherling, W.W. Neuromagnetic investigation of somatotopy of human hand somatosensory cortex. Exp. Brain Res., 1991, 87: 641-648.

Baumgartner, C. Sutherling, W.W., Di, S. and Barth, D.S. Spatiotemporal modeling of cerebral evoked magnetic fields to median nerve stimulation. Electroenceph. Clin. Neurophysiol., 1991, 79: 27-35.

Buchner, H., Adams, L., Knepper, A., Rüger, R., Laborde, G., Ludwig, I., Reul, J. and Scherg, M. Pre-operative determination of the central sulcus by dipole source analysis of early somatosensory evoked potentials and 3D-NMR-tomography. J. Neurochir., in press.

Buchner, H., Adams, L., Müller, A., Ludwig, I., Knepper, A., Thron, A., Niemann, K. and Scherg, M. Somatotopy of human hand somatosensory cortex revealed by dipole source analysis of early somatosensory evoked potentials and 3D-NMR-tomography. Electroenceph. Clin. Neurophysiol., in press.

Buchner, H. and Scherg, M. Analyse der Generatoren früher kortikaler somatosensibel evozierter Potentiale (N. medianus) mit der Dipolquellenanalyse: Erste Ergebnisse. Z. EEG-EMG, 1991, 22: 52-69.

Broughton, R.J. Discussion. In: E. Donchin and D.B. Lindsley (Eds.), Average evoked potentials (NASA SP-191), US Government printing office, Washington, 1969: 79-84.

Cheron, G. and Borenstein, S. Specific gating of the early somatosensory evoked potentials during active movement. Electroenceph. Clin. Neurophysiol., 1987, 67: 537-548.

Cheron, G. and Borenstein, S. Mental movement simulation affects the N30 frontal component of the somatosensory evoked potentials. Electroenceph. Clin. Neurophysiol., 1992, 84: 288-292.

Cohen, D. and Cuffin, B.N. Demonstration of useful differences between magnetoencephalogram and electroencephalogram. Electroenceph. Clin. Neurophysiol., 1983, 56: 38-51.

Cohen, D., Cuffin, B.N., Yunokuchi, K., Maniewski, R., Purcell, C., Cosgrove, G.R., Ives, J., Kennedy, J.G. and Schomer, D.L. MEG versus EEG localization test using implanted sources in the human brain. Ann. Neurol., 1990, 28: 811-817.

Cuffin, B.N. and Cohen, D. Comparison of the magnetoencephalogram and electroencephalogram. Electroenceph. Clin. Neurophysiol., 1979, 47: 132-146.

Cuffin, B.N., Cohen, D., Yunokuchi, K., Maniewsi, R., Purcell, C., Cosgrove, G.R., Ives, J., Kennedy, J. and Schomer, D. Tests of EEG localisation accuracy using implanted sources in the human brain. Ann. Neurol., 1991, 29: 132-138.

Desmedt, J.E. Somatosensory Evoked Potential. In: T.W. Picton (Ed.), EEG-Handbook. vol 3. Human Event - Related Potentials, Elsevier, New York, Amsterdam, 1988: 245-360.

Desmedt, J.E. and Tomberg, C. Mapping early somatosensory evoked potentials in selective attention: critical evaluation of control conditions used for titrating by difference the cognitive P30. P40. P100 and N140. Electroenceph. Clin. Neurophysiol., 1989, 74: 321-346.

Dössel, M., David, B., Fuchs, M., Krüger, J., Kullmann, W.H. and Lüdeke, K.M. A modular approach to multichannel magnetometery. Clin. Phys. Physiol. Meas., 1991, 12: 75-79.

Dössel, O., David, B., Fuchs, M., Krüger, J., Kullmann, W.H. and Lüdeke, K.M. A modular 19-channel SQUID system for biomagnetic measurements. In: H. Koch and H. Lübbig (Eds.), Proc. in Phys. Supercond. devices and their appl., 1992, Vol. 64: 517-520.

Dössel, O., David, M., Fuchs, M., Küger, J., Lüdeke, K.M. and Wischmann, H.-A. A 31-channel SQUID system for biomagnetic measurements. Applied Superconductivity, 1993, Vol. 1, No. 10-12: 1813-1825.

Ebeling, U., Schmidt, U.D. and Reulen, H.J. Tumor-surgery within the central motor strip: surgical results with the aid of electrical motor cortex stimulation. Acta Neurochir., 1989, 101: 100-107.

Fender, D.H. Source localization of brain electrical activity. In: A.S. Gevins and A. Remond (Eds.), EEG Handbook, Vol. 1, Elsevier, New York, Amsterdam, 1987: 355-403.

Fender, D.H. Models of the human brain and the surrounding media: their influence on the reliability of source localization. J. Clin. Neurophysiol., 1991, 8: 381-390.

Franssen, H., Stegeman, D.F., Moleman, J. and Schoobaar, R.P. Dipole modelling of median nerve SEPs in normal subjects and patients with small subcortical infarcts. Electroenceph. Clin. Neurophysiol., 1992, 84: 401-417.

Freeman, W.J. Mass action in the nervous system. Academic Press, New York, 1975: 1-489.

Fuchs, M. and Dössel, O. Online head position determination for MEG-measurement. In: M. Hoke, S.N. Erne, Y.C. Okada and G.L. Romani (Eds.), Biomagnetism: Clinical Aspects, Elsevier, New York, Amsterdam, 1992: 869-873.

Fuchs, M., Wischmann, H.-A. and Dössel, O. Overlay of neuromagnetic current density images and morphological MR images. SPIE., 1992, 1808: 676-684.

Fuchs, M., Wischmann, H.-A. and Dössel, O. Overlay of biomagnetic current reconstructions and morphological MR images. IEEE. Proc. Neuroscience and Technology, Lyon, 1992: 56-59.

Giard, M.H., Peronnet, F., Pernier, J., Mauguière, F. and Bertrand, O. Sequential color mapping system of brain potentials. Comput. Methods Progr. Biomed., 1982, 20: 9-16.

Hari, R. On brains magnetic responses to sensory stimuli. J. Clin. Neurophysiol., 1991, 8: 157-169.

Hari, R., Hämäläinen, M., Ilmoniemi, R. and Lounasmaa, O.V. MEG versus EEG localization test. Ann. Neurol., 1991, 30: 222-223.

Lehmann, D. Principles of spatial analysis. In: A.S. Gevins and A. Rémond (Eds.), EEG Handbook (Methods of analysis of brain electrical and magnetic signals), Elsevier, New York, Amsterdam, 1987: 309-354.

Lopes da Silva, F.H., Wieringa, H.J. and Peters, M.J. Source localization of EEG versus MEG: Empirical comparison using visually evoked responses and theoretical considerations. Brain Topography, 1991, 4: 133-142.

Lüders, H., Dinner, D.S., Lesser, R.P. and Morris, H.H. Evoked potentials in cortical localization. J. Clin. Neurophysiol., 1986, 3: 75-84.

Lüders, H., Lesser, R.P., Hahn, J., Dinner, D.S. and Klem, G. Cortical somatosensory evoked potentials in response to hand stimulation. J. Neurosurg., 1983, 58: 885-894.

Nunez, P.L. Localization of brain activity with electroencephalography. In: S. Sato (Ed.), Magnetoencephalography (Advances in Neurology) Vol. 54, Raven Press, New York, 1990: 39-65.

Reilly, A.J., Hallet, M., Cohen, L.G., Tarkka, I.M. and Dang, N. The N30 component of somatosensory evoked potentials in patients with dystonia. Electroenceph. Clin. Neurophysiol., 1992, 84:,243-247.

Rossini, P.M., Babiloni, F., Bernardi, G., Cecchi, L., Johnson, P.B., Malentacca, A., Stanzione, P. and Urbano, A. Abnormalities of short-latency somatosensory evoked potentials in parkinsonian patients. Electroenceph. Clin. Neurophysiol., 1989, 74: 277-289.

Scherg, M. Fundamentals of dipole source potential analysis. In: F. Grandori, M. Hoke and G.L. Romani (Eds.), Auditory evoked magnetic fields and electric potentials (Advances in Audiology) Vol. 6, Karger, Basel, Switzerland, 1990: 40-69.

Scherg, M. Functional imaging and localization of electromagnetic brain activity. Brain Topography, 1992, 5: 103-112.

Scherg, M. and Berg, P. Use of prior knowledge in brain electromagnetic source analysis. Brain Topography, 1991, 4: 143-150.

Scherg, M. and von Cramon,D. Two bilateral sources of the late AEP as identified by a spatio-temporal dipole model. Electroenceph. Clin. Neurophysiol., 1985, 62: 32-44.

Tiihonen, J., Hari, R. and Hämäläinen, M. Early deflections of cerebral magnetic responses to median nerve stimulation. Electroenceph. Clin. Neurophysiol., 1989, 74: 290-296.

van Oosterom, A. History and evaluation of methods for solving the inverse problem. J. Clin. Neurophysiol., 1991, 8: 371-380.

Williamson, S.J. MEG versus EEG localization test. Ann. Neurol., 1991, 30: 222.

Wood, C.C., Cohen, D., Cuffin, B.N., Yarita, M. and Allison, T. Electrical sources in human somatosensory cortex: identification by combined magnetic and potential recordings. Science, 1985, 227: 1051-1053.